

# Stacked Autoencoder Based Multi-Omics Data Integration for Cancer Survival Prediction

Xing Wu, Qiulian Fang

**Abstract**—Cancer survival prediction is important for developing personalized treatments and inducing disease-causing mechanisms. Multi-omics data integration is attracting widespread interest in cancer research for providing information for understanding cancer progression at multiple genetic levels. Many works, however, are limited because of the high dimensionality and heterogeneity of multi-omics data. In this paper, we propose a novel method to integrate multi-omics data for cancer survival prediction, called Stacked AutoEncoder-based Survival Prediction Neural Network (SAEsurv-net). In the cancer survival prediction for TCGA cases, SAEsurv-net addresses the curse of dimensionality with a two-stage dimensionality reduction strategy and handles multi-omics heterogeneity with a stacked autoencoder model. The two-stage dimensionality reduction strategy achieves a balance between computation complexity and information exploiting. The stacked autoencoder model removes most heterogeneities such as data's type and size in the first group of autoencoders, and integrates multiple omics data in the second autoencoder. The experiments show that SAEsurv-net outperforms models based on a single type of data as well as other state-of-the-art methods. The source code can be found on the Github: <https://github.com/luckydoggy98/SAEsurv-net>.

**Index Terms**—Cancer Survival Prediction, Stacked Autoencoder, Multi-Omics Data Integration.

## 1 INTRODUCTION

LOOKING back to the previous decade, feeding integrating multi-omics data and clinical data as input to models leads to a significant increase in accuracy of survival prediction, which facilitates understanding biological processes of disease and personalizing optimal therapies. Cancer is associated with abnormal cell growth, uncontrollable cell division and other tissues of the body through metastasis. The onset and progression of cancer can occur under the influence of complicated mechanisms and alterations at various levels including genome, proteome, transcriptome, and metabolome etc. [1]. Therefore, integration strategies across multiple cellular function levels provide unprecedented opportunities to understand the underlying biological mechanisms of cancer [2].

The term "multi-omics" refers to the study of the genome, transcriptome, epigenome, proteome, exposome, and microbiome [3]. Specifically, genomics is the study of identifying genetic variants associated with disease at the genome scale. Transcriptomics is the study of RNA expression from specific tissues, which provides information about cell- and tissue-specific gene expression. Epigenomics are concerned with the genome-wide characterization of DNA methylation or post-translational histone modifications capable of imposing stable and heritable changes in a gene without changing the DNA sequence. Metabolomics provides a snapshot of an organism's or tissue's metabolic state.

Proteomics is the qualitative and quantitative study of the proteome. Exposomes are non-genetic disease drivers that represent the totality of environmental exposure throughout a person's life. Microbiomes are microorganisms influencing the physiology of an individual, such as bacteria, viruses, and fungi [3]. High-throughput experimental technologies, including next-generation sequencing, microarrays, and RNA-sequencing technologies provide exponentially increased amount of available omics data [4]. Combining properly these types of omics data as predictor variables allows to comprehensively model biological variation at various levels of regulation [5].

However, challenges such as the curse of dimensionality and data heterogeneity arise when integrating multi-omics data. Because of the large number of measured objects and the small number of patients, the curse of dimensionality occurs naturally in omics data. After integrating, the situation worsens because the number of features to be analyzed grows while the number of samples remains constant. This often arises the risk of overfitting [6]. The heterogeneity of multi-omics data is on account of different number of features, mismatched data distributions, scalings and modalities between various omics [7]. These discrepancies between omics can hinder their integration.

Recent researches mainly focus on addressing these challenges. Dimensionality reduction techniques are used in two ways: feature selection, which identifies a relevant subset of the original features, and feature extraction, which projects data from a high-dimensional space to a lower-dimensional space [8]. Feature selection methods can be classified into three main types: (1) filter-based, (2) wrapper-based, (3) embedded methods. Filter-based methods are independent of any predictive model and implement statistical analysis to

- X. Wu is with the Department of mathematics and statistics, Central South University, Changsha, HN 410083, China.  
E-mail: wuxing98@csu.edu.cn
- Q. Fang is with the Department of mathematics and statistics, Central South University, Changsha, HN 410083, China.  
E-mail: qiulianfang@csu.edu.cn

Manuscript received. . .

select a subset of relevant features based on correlation (e.g., CFS [9]), distance (e.g., ReliefF [10]), information gain (e.g., mRMR [11]) and statistical test [12]. Wrapper-based methods try to search the best subset of features by applying predictive model repeatedly on different set of features, and then keep the best performing subsets (e.g., RFE [13]), but this strategy is limited by its computing efficiency especially when the dataset is large. Embedded methods are algorithms with feature selection built directly in the predictive models (e.g., tree based feature importance [14], LASSO). The most widely used feature extraction method is Principal Component Analysis (PCA) [15], which transforms high-dimensional features to linearly uncorrelated new features named principal components. However, the transformation in PCA is a linear combination, so that PCA cannot handle non-linear trends in data. Autoencoder is a nonlinear feature transformation technique with multi-layer neural networks structures to extract latent features in a bottleneck layer, which can be employed to reduce dimensionality by restricting the number of bottleneck layer nodes [3]. Both feature selection and feature extraction methods can be used in the data integration analysis, either separately on each omics dataset before integrating or on concatenated multi-omics datasets. Selecting or extracting features from separate datasets before integrating reduces the computation complexity of the subsequent analysis, but it ignores the relationship between the datasets and commonly results in unwanted redundancy and suboptimal results [16]. When dealing with concatenated datasets, it is possible to capture information shared across different datasets and discover more revelatory features that single-omics would miss. However, it must deal with a high-dimensional input data matrix. In order to achieve a balance between computation efficiency and information exploitation quality, the dimensionality reduction is expected to combine with the data integration to be a syncretic process.

M. Picard *et al.* classify integration methods into five types: early (concatenation-based), mixed (transformation-based), late (model-based), intermediate and hierarchical [17]. The early integration is based on concatenating every dataset into a single large matrix [18]. Although simple, this process results in a more complex, noisier and higher dimensional matrix, and ignores the specific data distribution of each omics [17]. The mixed strategy addresses the shortcomings of the early integration by independently transforming each dataset into a simpler representation before concatenating, which can be less dimensional and less noisy [17]. Commonly used transformation methods are kernel-based, graph-based and neural network-based. Artificial neural networks can capture nonlinear and hierarchical new features from the hidden layers due to their multi-layered structures and nonlinear activation functions, which process can be considered as successive feature extraction. Z Huang *et al.* propose an algorithm called SALMON to represent mRNA-seq and miRNA-seq data with neural networks respectively. Then the output layers of these networks are fed into a full connected layer together to predict death risk [19]. Some neural networks have architectures specialized in learning meaningful representation, such as autoencoder. New representations for each dataset can be extracted by type-specific encoding sub-networks [20], [21]. Intermediate

integration can be described as any methods capable of jointly integrating the multi-omics datasets without prior transformation [17]. For example, K Chaudhary *et al.* feed stacked three omics data matrices into an autoencoder to extract new integrated features [22]. H Torkey *et al.* train autoencoder based on concatenated data and take the decoder layer as the new features [23]. Similar to the early integration, the large input matrix in intermediate integrating process is also difficult to exploit. Late integration means to apply predictive models separately on each dataset and then combines their predictions [17]. Sun *et al.* use a set of deep neural networks to extract information from different datasets respectively, then conduct a score-level fusion for the results predicted by each DNN model [24]. The limitation of this strategy is that it cannot capture inter-omics interactions since it only combines predicted results [17]. Hierarchical integration strategy bases the integration on inclusion of the prior knowledge of regulatory relationships between different datasets, which means external information from interaction database and scientific literature is used [17]. For example, J Hao *et al.* propose a neural network named MiNet, which has a structure following a biological system by utilizing prior knowledge of biology pathways [25]. On the one hand, this strategy improves model interpretability; on the other hand, its reliance on prior knowledge limits its ability to investigate new biological mechanisms.

Inspired by successful use of integrating strategies in multi-omics data analysis, particularly the use of the neural networks for dimensionality reduction and data integration, we propose a novel approach to integrate multi-omics data for survival analysis called Stacked AutoEncoder based survival prediction neural network (SAEsurv-net). The main contributions of this paper can be summarized as follows: (1) achieving a balance between computation complexity and information exploiting by applying a two-stage dimensionality reduction strategy that first removes features irrelevant to the survival outcome for each data type and then combines the remaining features from various data types; (2) handling heterogeneity of multiple data types by introducing a stacked autoencoder model, in which most heterogeneities such as data's type and size are removed in the first group of autoencoders; (3) comparing the performance of SAEsurv-net with neural network models based on a single data type and other previous state-of-the-art models.

The rest of the paper is organized as follows: Section 2 elaborates the overall approach, including data collection and preprocessing, as well as the construction of the SAEsurv-net. Section 3 shows the experimental settings and results. Section 4 summarizes the research, identifies potential limitations, and suggests future directions.

## 2 METHODS AND MATERIALS

### 2.1 Materials

To evaluate the performance of SAEsurv-net, we download glioblastoma multiforme (GBM), ovarian serous cystadenocarcinoma (OV), and breast invasive carcinoma (BRCA) datasets from The Cancer Genome Atlas (TCGA) project through UCSC Xena [26]. Each dataset contains three types

TABLE 1  
The characteristics of the data

Disease	Data Category	Number of Samples	Number of Features	Number of Features after Preprocess	Number of Features after SAE
GBM	gene	156	60484	4080	totally 400
	cnv		19730	238	
	clinical		3	2	
OV	gene	373	60484	3503	totally 365
	cnv		19730	1075	
	clinical		5	2	
BRCA	gene	1040	60484	5313	totally 595
	cnv		19730	1042	
	clinical		9	3	

of information: gene expression, copy number variations (CNV), and clinical information. Gene expression features are taken as FPKM values from the Illumina platform. CNV features are derived from Affymetrix Genome Wide Human SNP 6.0 platform. Characteristics for each dataset are shown in Table 1. Each gene expression dataset has 60484 features, each CNV dataset has 19730 features, and each clinical dataset of GBM, OV, and BRCA has 3, 5, and 9 features, respectively. Features involved in each clinical dataset are listed in Appendix A. After removing the patients who do not have all the three types of information simultaneously, we get 156, 373, 1040 samples in GBM, OV, BRCA data respectively.

## 2.2 Preprocess

In the first place, We normalize all datasets and remove redundant features. In gene expression data, features are applied  $\log 2(1 + x)$  transformation and zero-mean unit-variance normalization. In clinical data, categorical features are transformed into one-hot codes and numerical features are normalized to zero-mean unit-variance, while the missing values are imputed by mode.

To avoid overfitting, we adopt a two-stage dimensionality reduction strategy. In the first stage, we remove features with zero variance and features with the same value for each type of data. After that, the log-rank test is applied to each feature, and features with the p-values greater than 0.05 are removed. Before the log-rank test, features in gene expression are discretized into three categories: under-expression (-1), over-expression (1), and baseline (0), and numerical values are used after the test. The results of this stage are shown in Table 1. For all diseases, the decrease of the numbers of features in gene expression and CNV is greater than 90%. In the second stage, we apply a stacked autoencoder model to extract and integrate features from multiple omics data.

## 2.3 A Stacked Autoencoder Model for Feature Extraction and Integration

After the first stage of dimensionality reduction, we obtain a subset of original features for each single dataset, however, the number of features is still too large when compared with the sample size. In the second stage, we create a lower-dimensional representation for multiple omics with a stack of autoencoder models. This procedure can be divided into two steps. The first step is to train an autoencoder on each dataset. By limiting the number of nodes in the

bottleneck layer, a lower-dimensional representation of each dataset can be obtained. In the new representations, most heterogeneities such as data’s type and size are removed. In the second step, representations corresponding to multiple omics data are concatenated and fed into another autoencoder. This step simultaneously reduces dimensionality and integrates data. Consequently, a cross-omics representation is obtained.

As shown in Fig. 1, the preprocessed gene expression vector  $x_{\text{gene}}$  and CNV vector  $x_{\text{cnv}}$  are fed into two autoencoder models, respectively. Each autoencoder is a neural network that is trained to attempt to copy its input  $x$  to its output  $\hat{x}$  [27]. The network consists of two parts: an encoder that represents the input and a decoder that produces a reconstruction. The most salient features of the training data will be captured by constraining the bottleneck layer  $h$  to have a smaller dimension than  $x$ . Let  $h_{\text{gene}}$  and  $h_{\text{cnv}}$  denote the hidden representations of the two one-hidden-layer autoencoder models respectively:

$$h_{\text{gene}} = f_{1,g}(W_g x_{\text{gene}} + b_g) \quad (1)$$

$$h_{\text{cnv}} = f_{1,c}(W_c x_{\text{cnv}} + b_c) \quad (2)$$

And the reconstruction is:

$$\hat{x}_{\text{gene}} = g_{1,g}(W'_g h_{\text{gene}} + b'_g) \quad (3)$$

$$\hat{x}_{\text{cnv}} = g_{1,c}(W'_c h_{\text{cnv}} + b'_c) \quad (4)$$

Then the two hidden representations are concatenated as  $[h_{\text{gene}}; h_{\text{cnv}}]$  and inputted to another autoencoder, which extracts the cross-omics representation  $h_{\text{con}}$  of multiple omics data:

$$h_{\text{con}} = f_2(W_{\text{con}}[h_{\text{gene}}; h_{\text{cnv}}] + b_{\text{con}}) \quad (5)$$

And the reconstruction is:

$$\hat{x}_{\text{con}} = g_2(W'_{\text{con}} h_{\text{con}} + b'_{\text{con}}) \quad (6)$$

This two-step data extraction process based on a stack of autoencoder models is a so-called Stacked AutoEncoder (SAE) model [28]. SAE is defined as a stacking of multiple autoencoder models to form a deep structure. In SAE, the hidden layer of the  $k$ th autoencoder is fed as the input into the  $(k + 1)$ th autoencoder.

We define regularized mean squared error (MSE) loss as the objective function for each autoencoder:

$$L_g(W_g, b_g, W'_g, b'_g) = \sum_{i=1}^n \|\hat{x}_{\text{gene}}^i - x_{\text{gene}}^i\|_2^2 + \lambda_g(\|W_g\|_1 + \|W'_g\|_1) + \alpha_g(\|W_g\|_2^2 + \|W'_g\|_2^2) \quad (7)$$

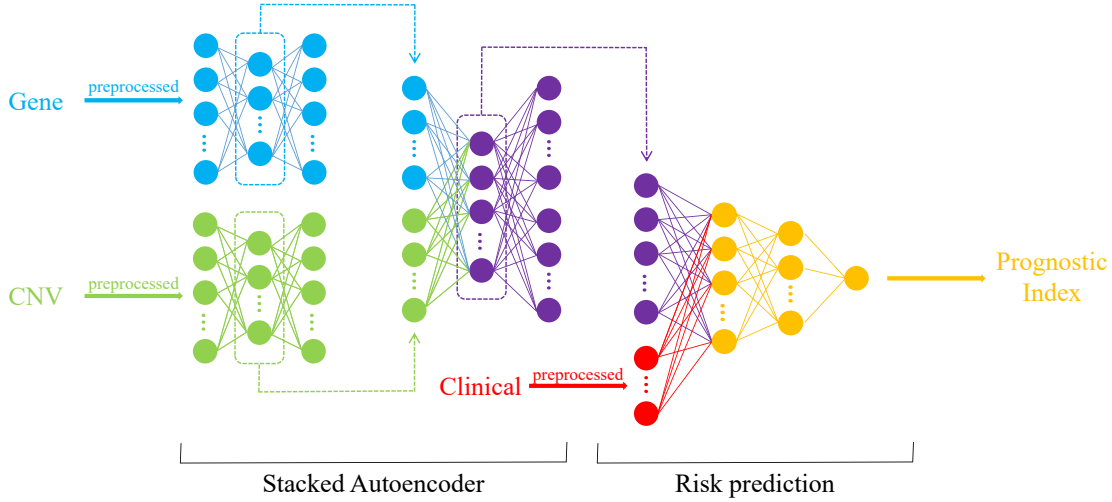


Fig. 1. Architecture of SAEsurv-net. In the first place, gene expression (Gene), copy number variations (CNV) and clinical data are preprocessed. In this process, all features are normalized and redundant features are removed. Next, the preprocessed gene expression and CNV vectors are fed into two one-hidden-layer autoencoder models respectively. From these models, the low-dimensional representations for corresponding data can be obtained. Then, the representations are concatenated and fed into another one-hidden-layer autoencoder. After that, a cross-omics representation is obtained. Subsequently, the cross-omics representation is combined with clinical vector and inputted to a risk prediction network with two hidden layers. The final outcome of the risk prediction network is Prognostic Index (PI), indicating the death risk of samples.

$$L_c(W_c, b_c, W'_c, b'_c) = \sum_{i=1}^n \|\hat{x}_{\text{cnv}}^i - x_{\text{cnv}}^i\|_2^2 + \lambda_c(\|W_c\|_1 + \|W'_c\|_1) + \alpha_c(\|W_c\|_2^2 + \|W'_c\|_2^2) \quad (8)$$

$$L_{\text{con}}(W_{\text{con}}, b_{\text{con}}, W'_{\text{con}}, b'_{\text{con}}) = \sum_{i=1}^n \|\hat{x}_{\text{con}}^i - [h_{\text{gene}}^i; h_{\text{cnv}}^i]\|_2^2 + \lambda_{\text{con}}(\|W_{\text{con}}\|_1 + \|W'_{\text{con}}\|_1) + \alpha_{\text{con}}(\|W_{\text{con}}\|_2^2 + \|W'_{\text{con}}\|_2^2) \quad (9)$$

where  $\|\cdot\|_1$  and  $\|\cdot\|_2^2$  denote  $L_1$  and  $L_2$  norm, and  $i$  denotes the  $i$ th feature. The weight parameters  $W_g, W'_g, W_c, W'_c, W_{\text{con}}, W'_{\text{con}}$  and bias parameters  $b_g, b'_g, b_c, b'_c, b_{\text{con}}, b'_{\text{con}}$  in neural networks can be obtained by minimizing the loss functions respectively, the hyperparameters such as activation function, numbers of nodes,  $\alpha_g, \lambda_g$ , etc., can be obtained by optimizing algorithm described in Section 3.1.

## 2.4 A Risk Prediction Neural Network Model for Survival Analysis

Once the stack of autoencoder models has been built, its highest level output representation  $h_{\text{con}}$  can be used in the following prediction. As shown in Fig. 1, the vector  $x_{\text{in}}$ , which is a concatenation of  $h_{\text{con}}$  and clinical vector  $x_{\text{cli}}$ , is inputted to a risk prediction network with two hidden layers. The final outcome of the risk prediction network is Prognostic Index (PI), which is a linear combination of the neurons in the previous layer. PI is introduced to the hazard function  $h(t|x_{\text{in}})$  for the Cox proportional hazards model as an estimate of risk function [25]:

$$h(t|x_{\text{in}}) = h_0(t)\exp(\text{PI}) \quad (10)$$

where  $x_{\text{in}} = [h_{\text{con}}; x_{\text{cli}}]$ , and  $h_0(t)$  is the baseline hazard function which can be an arbitrary non-negative function of time. This hazard function shows the death rate at time

$t$  conditional on survival until time  $t$  or later. We can say that samples with higher PI have higher death risk. The loss function of the risk prediction network is the regularized negative log partial likelihood:

$$L_r(\Theta_r) = - \sum_{i:\delta_i=1} \left( \text{PI}_{\Theta_r}(x_{\text{in},i}) - \log \sum_{j \in \mathfrak{R}(T_i)} e^{\text{PI}_{\Theta_r}(x_{\text{in},j})} \right) + \lambda_r \|W_r\|_1 + \alpha_r \|W_r\|_2^2 \quad (11)$$

where  $T_i, E_i, \mathfrak{R}(T_i)$  denotes the death time, censored status and risk set for the  $i$ th death, respectively.  $\delta_i = 1$  means the death time of the  $i$ th sample is observed, and  $\delta_i = 0$  means the death time of the  $i$ th sample is censored. Then  $\Theta_r = \{W_r, b_r\}$  can be obtained by minimizing the loss function, and the hyperparameters such as activation function, numbers of nodes,  $\alpha_r, \lambda_r$ , etc., can be obtained by the optimizing algorithm described in Section 3.1.

## 3 RESULTS

### 3.1 Experimental Design

The performance of SAEsurv-net is assessed by comparing it with networks based on a single data type and current state-of-the-art methods, such as DeepSurv [29]. We consider C-index [30] as the measurement of the predictive performance. It is defined as the ratio of the concordant predicted pairs to the total comparable pairs:

$$c = \frac{1}{\text{num}} \sum_{i:\delta_i=1} \sum_{j:y_i < y_j} I[\text{PI}_i > \text{PI}_j] \quad (12)$$

where num denotes the total number of comparable pairs,  $I[\cdot]$  is the indicator function.  $\delta_i, y_i$  and  $\text{PI}_i$  denote the censored status, observed survival time and predicted death risk of the  $i$ th sample.

We repeat the evaluation 20 times for the reproducibility of the model performance. On each experiment, data is

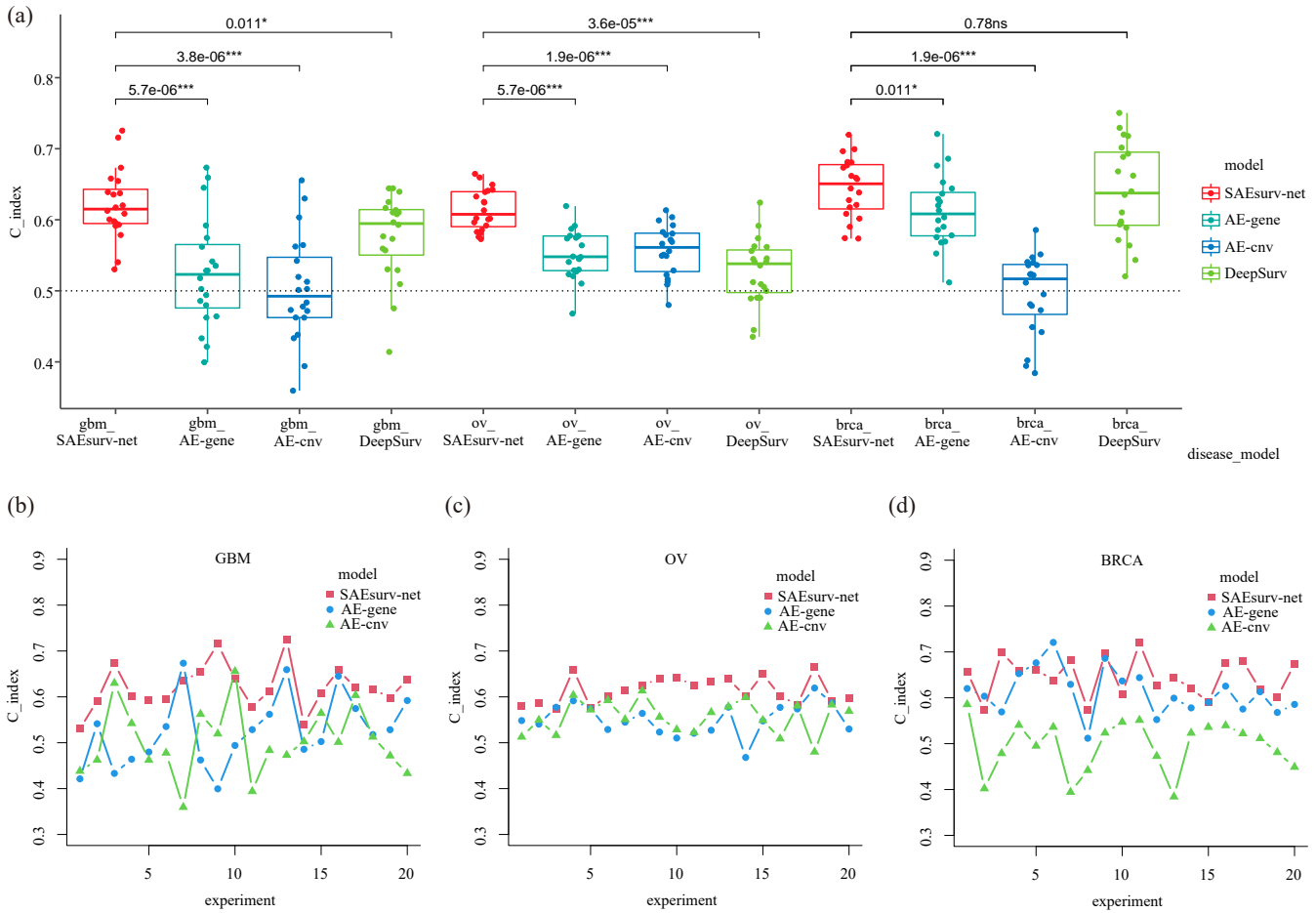


Fig. 2. C-index in 20 experiments. (a) Box plots of C-index in 20 experiments. Wilcoxon test results are represented by p-values and symbol \*. \*\*\* denotes a p-value lower than 0.001, \*\* denotes a p-value bigger than 0.001 but lower than 0.01, \* denotes a p-value bigger than 0.01 but lower than 0.05, ns denotes a p-value bigger than 0.05. (b),(c) and (d) C-index in each experiment for GBM, OV and BRCA.

randomly split into two subsets: training (80%) and test data (20%) by stratified sampling with censored status. We train every model with training data, and apply a 5-fold cross validation to find the optimal hyperparameters. Once the model was well-trained, the test data is used to evaluate the predictive performance.

The neural networks are implemented based on TensorFlow 1.15.2 and Keras 2.8.0 deep learning library; the data preprocessing and train-test split are implemented with scikit-learn [31]; the log rank test and C-index computation are performed with lifelines [32]; the plots of results are accomplished through ggplot2 [33] and ggpubr with Rstudio. More details of SAEsurv-net can be found at <https://github.com/luckydoggy98/SAEsurv-net>. In order to achieve a nearly fair comparison, we train DeepSurv by following the implementation codes provided by the authors' GitHub <https://github.com/jaredleekatzman/DeepSurv>.

We perform the hyperparameter optimization through Bayesian optimization implemented with BayesianOptimization [34] and NNI [35]. The latter is an open source AutoML toolkit for hyperparameter optimization, neural architecture search, model compression and feature engineering. For autoencoder models, the configuration with the least validation mean squared error will be chosen, for

risk prediction network, the configuration with the largest validation C-index will be chosen. The detailed hyperparameters used in SAEsurv-net are described in Appendix B.

### 3.2 Comparison of SAEsurv-net with Single-Omics Data Based Models

To illustrate the effectiveness of integration strategy, we compare the performance of SAEsurv-net with neural networks based on a single type of data. For simplicity, we denote networks only based on gene expression or CNV data as AE-gene and AE-cnv, respectively. In AE-gene or AE-cnv, preprocessed gene expression or CNV data is fed into a one-hidden-layer autoencoder, as in SAEsurv-net. Then the representations extracted are fed into a two-hidden-layer risk prediction network. There is no integrating step in AE-gene nor AE-cnv. The loss functions and hyperparameter optimization methods in AE-gene, AE-cnv, and SAEsurv-net are the same.

Fig. 2(a) shows the distribution of C-index of the experiments. The mean values of C-index are listed in Table 2. For each disease, SAEsurv-net achieves the highest mean (0.6212, 0.6141, and 0.6451 respectively) and relatively low variance of C-index, compared with AE-gene (0.5250, 0.5516,

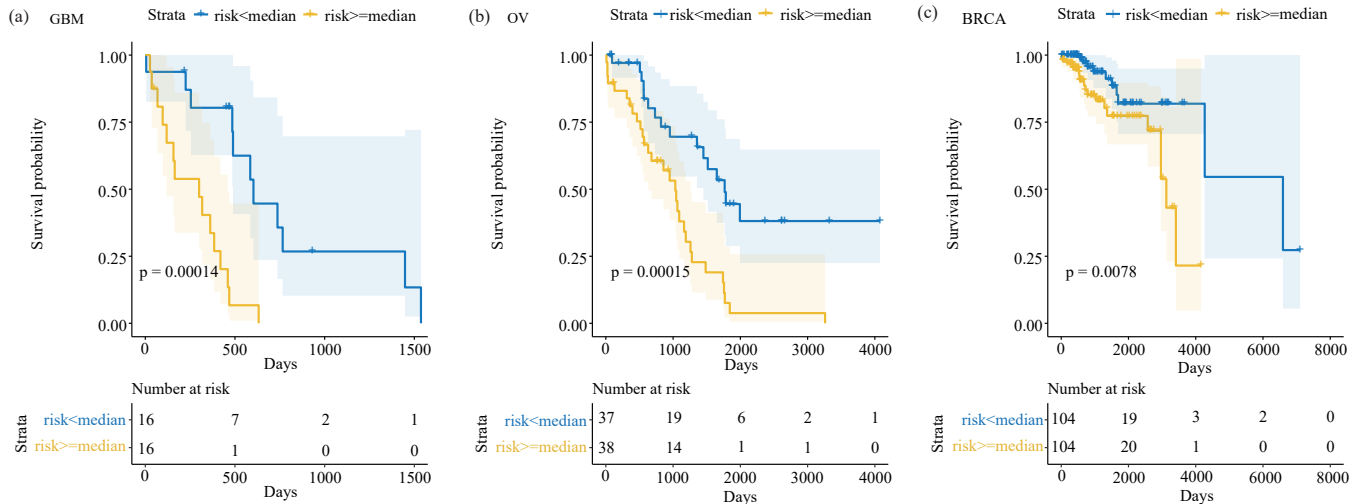


Fig. 3. Kaplan-Meier plots for risk predicted by SAEsurv-net in (a) GBM, (b) OV, and (c) BRCA dataset. For each test data, samples with the predicted risk lower than the overall median of predicted risk are assigned to the low-risk group, otherwise they are assigned to the high-risk group. Tables below present the number of samples belonging to the low- and high-risk groups at certain times.

and 0.6119 respectively) and AE-cnv (0.5025, 0.5566, and 0.4958 respectively). \* in Fig. 2(a) denotes the Wilcoxon rank-sum test results for two groups of C-index. \*\*\* denotes a p-value less than 0.001, \*\* denotes a p-value greater than 0.001 but less than 0.01, \* denotes a p-value greater than 0.01 but less than 0.05, ns denotes a p-value greater than 0.05. We can see that the outperformance of SAEsurv-net against AE-gene and AE-cnv is statistically significant ( $p$ -value < 0.05). As shown in Fig. 2(b)(c)(d), SAEsurv-net has the highest C-index in almost every experiment. It means that the performance improvement of SAEsurv-net is consistent and does not rely on data splitting.

TABLE 2  
Mean values of C-index over 20 experiments

Disease	Model	C-index mean
GBM	AE-gene	0.5250
	AE-cnv	0.5025
	DeepSurv	0.5763
	<b>SAEsurv-net</b>	<b>0.6212</b>
OV	AE-gene	0.5516
	AE-cnv	0.5566
	DeepSurv	0.5277
	<b>SAEsurv-net</b>	<b>0.6141</b>
BRCA	AE-gene	0.6119
	AE-cnv	0.4958
	DeepSurv	0.6395
	<b>SAEsurv-net</b>	<b>0.6451</b>

### 3.3 Comparison of SAEsurv-net with Other Methods

To demonstrate the outperformance of SAEsurv-net against other integration strategies, We compare the performance of SAEsurv-net with DeepSurv. As shown in Table 2 and Fig. 2(a), for GBM and OV data, SAEsurv-net has higher C-index means (0.6212 and 0.6141) than DeepSurv with the p-values less than 0.05. It means that SAEsurv-net significantly outperforms DeepSurv on these two datasets. For BRCA data, the p-value of test between SAEsurv-net and DeepSurv is greater than 0.05, which means there is no significant improvement of SAEsurv-net against DeepSurv.

However, SAEsurv-net still holds a higher mean (0.6451) and lower variance of C-index, indicating that it performs more robustly than DeepSurv at the same accuracy level.

### 3.4 Visualization of risk prediction with Kaplan-Meier plot

We perform the Kaplan-Meier plot with log-rank test to visualize the risk prediction of SAEsurv-net in one experiment. For a specific disease, samples in the test set are grouped into low-risk and high-risk groups according to their predicted risk. Specifically, samples with predicted risk lower than the overall median of predicted risk are assigned to the low-risk group, otherwise they are assigned to the high-risk group. Fig. 3 shows the Kaplan-Meier plots of the three diseases. We can see the distinct separation of the two groups with significant log-rank test results ( $p$ -value < 0.01).

## 4 DISCUSSION AND CONCLUSION

Cancer survival prediction is important for developing personalized treatments and inducing disease-causing mechanisms. In this study, we established a novel neural network named SAEsurv-net to integrate multi-omics data and predict death risk of patients with cancer. SAEsurv-net addresses the curse of dimensionality with a two-stage dimensionality reduction strategy. In the first stage, irrelevant features in all datasets are removed. In the second stage, the remaining features are transformed and integrated into a lower-dimensional representation by a stack of autoencoder models. For details, SAE extracts type-specific representations for each dataset from the first autoencoder, then extracts cross-omics representation from the second autoencoder. Most heterogeneities such as data's type and size are removed through the first group of autoencoders. So SAEsurv-net also handles the heterogeneity between different types of data. Compared with integration strategies that either concatenating data matrices at the start or combining prediction results at the end, SAEsurv-net takes a middle ground approach. Experimental results of SAEsurv-net for

cancer survival prediction are promising, achieving a higher mean and lower variance of C-index when compared to the neural networks based on a single data type and other state-of-the-art models. The evaluation results demonstrate the effectiveness of data integration strategy and advantages of SAEsurv-net.

However, there are still some areas to be explored. Firstly, the sample size is still small when compared with the number of model parameters. Considering about the difficulty and cost of obtaining a large amount of data, methods should be developed to maximize the use of available data. Transfer learning is focusing on transferring the knowledge from some source tasks to a target task when the latter has fewer high-quality training data [36]. Existing multi-omics studies transfer knowledge by combining datasets from different diseases [37], or by finetuning pretrained neural networks built on unlabeled dataset using labeled dataset [38]. However, involving unfamiliar instances may introduce noise and proper instance selection principles need to be studied. Additionally, the lack of interpretability of deep neural networks hinders their application to real situations, and interpretable models should be established. Tree-based models and graph-based models [39] can provide explicit decision-making processes, which can generate intelligible rules. Introducing biological knowledge is also helpful to enhance the interpretability and reduce the overfitting risk of models [25].

## APPENDIX A FEATURES USED IN CLINICAL DATA

TABLE 3  
Features Used in Clinical Data

Disease	Feature name	Description
GBM	age at initial pathologic diagnosis	age at which a disease was first diagnosed
	radiation.therapy	the patient’s history of radiation therapy
	gender.demographic	gender
	age at initial pathologic diagnosis	age at which a disease was first diagnosed
OV	clinical.stage	stage group determined on the tumor, regional node and metastases and by grouping cases with similar prognosis for cancer
	neoplasm.histologic.grade	the degree of abnormality of cancer cells
	person.neoplasm.cancer.status	the state or condition of an individual’s neoplasm
	race.demographic	race based on the Office of Management and Budget categories
	age at initial pathologic diagnosis	age at which a disease was first diagnosed
	history of neoadjuvant treatment	the patient’s history of neoadjuvant treatment and the kind of treatment given prior to resection of the tumor
	menopause.status	the status of a woman’s menopause
	pathologic.M	code to represent the defined absence or presence of distant spread or metastases (M) to locations
	pathologic.N	codes that represent the stage of cancer based on the nodes present (N stage)
	BRCA	pathologic.T
BRCA	ethnicity.demographic	ethnicity based on the Office of Management and Budget categories
	race.demographic	race based on the Office of Management and Budget categories
	person.neoplasm.cancer.status	the state of an individual’s neoplasm

## APPENDIX B DETAILED PARAMETER CONFIGURATIONS OF MODELS

TABLE 4  
Parameter configurations of the autoencoder on gene expression data

hyperparameter	GBM	OV	BRCA
dropout rate	0.4567	0.3683	0.1694
bottleneck units	290	450	460
optimizer	adam	nadam	nadam
activation function	softsign	tanh	tanh
$\lambda_g$	0	0	0
$\alpha_g$	0	0	0.00001
learning rate	0.001	0.001	0.0001
training epoch	50	80	100
mini-batch size	30	100	60

TABLE 5  
Parameter configurations of the autoencoder on CNV data

hyperparameter	value		
	GBM	OV	BRCA
dropout rate	0.0220	0.1624	0.0385
bottleneck units	230	580	270
optimizer	adam	adamax	adam
activation function	selu	selu	tanh
$\lambda_c$	0	0	0
$\alpha_c$	0.0001	0	0
learning rate	0.01	0.01	0.0001
training epoch	60	80	100
mini-batch size	55	40	80

TABLE 6  
Parameter configurations of the autoencoder that integrates data

hyperparameter	value		
	GBM	OV	BRCA
dropout rate	0.1071	0.1515	0.0647
bottleneck units	400	365	590
optimizer	adamax	adam	rmsprop
activation function	softsign	softsign	tanh
$\lambda_{con}$	0	0	0
$\alpha_{con}$	0.00001	0	0
learning rate	0.01	0.01	0.001
training epoch	40	60	80
mini-batch size	40	80	120

TABLE 7  
Parameter configurations of the risk prediction network

hyperparameter	value		
	GBM	OV	BRCA
dropout rate 1	0.3307	0.1753	0.1294
dropout rate 2	0.3307	0.4039	0.2553
bottleneck units 1	60	195	315
bottleneck units 2	60	100	435
optimizer	nadam	rmsprop	nadam
activation function	sigmoid	tanh	sigmoid
$\lambda_r$	0.00001	0.01	0.0001
$\alpha_r$	0	0.001	0
learning rate	0.001	0.0001	0.0001
training epoch	10	70	90
mini-batch size	50	30	500

## ACKNOWLEDGMENTS

The corresponding author: Qiulian Fang (E-mail: qiulianfang@csu.edu.cn). The authors would like to thank Yuchen Li, for his advice through the process.

The results shown here are in whole or part based upon data generated by the TCGA Research Network: <https://www.cancer.gov/tcga>.

## REFERENCES

- [1] B. Arjmand, S. K. Hamidpour, A. Tayanloo-Beik *et al.*, "Machine learning: A new prospect in multi-omics data analysis of cancer." *Frontiers in Genetics*, vol. 13, pp. 824 451–824 451, 2022.
- [2] O. Menyhárt and B. Györfy, "Multi-omics approaches in cancer research with applications in tumor subtyping, prognosis, and diagnosis," *Computational and Structural Biotechnology Journal*, vol. 19, pp. 949–960, 2021.
- [3] M. Kang, E. Ko, and T. B. Mersha, "A roadmap for multi-omics data integration using deep learning," *Briefings in Bioinformatics*, vol. 23, no. 1, p. bbab454, 2022.
- [4] D. J. Rigden, X. M. Fernández-Suárez, and M. Y. Galperin, "The 2016 database issue of nucleic acids research and an updated molecular biology database collection," *Nucleic acids research*, vol. 44, no. D1, pp. D1–D6, 2016.
- [5] M. D. Ritchie, E. R. Holzinger, R. Li *et al.*, "Methods of integrating data to uncover genotype–phenotype interactions," *Nature Reviews Genetics*, vol. 16, no. 2, pp. 85–97, 2015.
- [6] P. Domingos, "A few useful things to know about machine learning," *Communications of the ACM*, vol. 55, no. 10, pp. 78–87, 2012.
- [7] B. Mirza, W. Wang, J. Wang *et al.*, "Machine learning and integrative analysis of biomedical big data," *Genes*, vol. 10, no. 2, p. 87, 2019.
- [8] L. Wang, Y. Wang, and Q. Chang, "Feature selection methods for big data bioinformatics: a survey from the search perspective," *Methods*, vol. 111, pp. 21–31, 2016.
- [9] M. A. Hall *et al.*, "Correlation-based feature selection for machine learning," 1999.
- [10] I. Kononenko, "Estimating attributes: Analysis and extensions of relief," in *European conference on machine learning*. Springer, 1994, pp. 171–182.
- [11] C. Ding and H. Peng, "Minimum redundancy feature selection from microarray gene expression data," *Journal of bioinformatics and computational biology*, vol. 3, no. 02, pp. 185–205, 2005.
- [12] B. Fu, P. Liu, J. Lin *et al.*, "Predicting invasive disease-free survival for early stage breast cancer patients using follow-up clinical data," *IEEE Transactions on Biomedical Engineering*, vol. 66, no. 7, pp. 2053–2064, 2018.
- [13] I. Guyon, J. Weston, S. Barnhill *et al.*, "Gene selection for cancer classification using support vector machines," *Machine learning*, vol. 46, no. 1, pp. 389–422, 2002.
- [14] E. Scornet, "Trees, forests, and impurity-based variable importance," *arXiv preprint arXiv:2001.04295*, 2020.
- [15] M. Ringnér, "What is principal component analysis?" *Nature biotechnology*, vol. 26, no. 3, pp. 303–304, 2008.
- [16] T. M. Tang and G. I. Allen, "Integrated principal components analysis," *Journal of Machine Learning Research*, vol. 22, no. 198, pp. 1–71, 2021.
- [17] M. Picard, M.-P. Scott-Boyer, A. Bodein *et al.*, "Integration strategies of multi-omics data for machine learning analysis," *Computational and Structural Biotechnology Journal*, vol. 19, pp. 3735–3746, 2021.
- [18] S. Yousefi, F. Amrollahi, M. Amgad *et al.*, "Predicting clinical outcomes from large scale cancer genomic profiles with deep survival models," *Scientific reports*, vol. 7, no. 1, pp. 1–11, 2017.
- [19] Z. Huang, X. Zhan, S. Xiang *et al.*, "Salmon: survival analysis learning with multi-omics neural networks on breast cancer," *Frontiers in genetics*, vol. 10, p. 166, 2019.
- [20] H. Sharifi-Noghabi, O. Zolotareva, C. C. Collins *et al.*, "Moli: multi-omics late integration with deep neural networks for drug response prediction," *Bioinformatics*, vol. 35, no. 14, pp. i501–i509, 2019.
- [21] M. R. Karim, G. Wicaksono, I. G. Costa *et al.*, "Prognostically relevant subtypes and survival prediction for breast cancer based on multimodal genomics data," *IEEE Access*, vol. 7, pp. 133 850–133 864, 2019.
- [22] K. Chaudhary, O. B. Poirion, L. Lu *et al.*, "Deep learning–based multi-omics integration robustly predicts survival in liver cancer," *Clinical Cancer Research*, vol. 24, no. 6, pp. 1248–1259, 2018.
- [23] H. Torkey, M. Atlam, N. El-Fishawy *et al.*, "A novel deep autoencoder based survival analysis approach for microarray dataset," *PeerJ Computer Science*, vol. 7, p. e492, 2021.
- [24] D. Sun, M. Wang, and A. Li, "A multimodal deep neural network for human breast cancer prognosis prediction by integrating multi-dimensional data," *IEEE/ACM transactions on computational biology and bioinformatics*, vol. 16, no. 3, pp. 841–850, 2018.
- [25] J. Hao, M. Masum, J. H. Oh *et al.*, "Gene-and pathway-based deep neural network for multi-omics data integration to predict cancer survival outcomes," in *International Symposium on Bioinformatics Research and Applications*. Springer, 2019, pp. 113–124.
- [26] M. Goldman, B. Craft, M. Hastie *et al.*, "The ucsc xena platform for public and private cancer genomics data visualization and interpretation," *bioRxiv*, 2019. [Online]. Available: <https://www.biorxiv.org/content/early/2019/09/26/326470>
- [27] I. Goodfellow, Y. Bengio, and A. Courville, *Deep Learning*. MIT Press, 2016, <http://www.deeplearningbook.org>.
- [28] Z. Wang, Y. Fu, and T. S. Huang, *Deep Learning Through Sparse and Low-Rank Modeling*. Academic Press, 2019.
- [29] J. L. Katzman, U. Shaham, A. Cloninger *et al.*, "DeepSurv: personalized treatment recommender system using a cox proportional hazards deep neural network," *BMC medical research methodology*, vol. 18, no. 1, pp. 1–12, 2018.

- [30] H. Uno, T. Cai, M. J. Pencina *et al.*, "On the c-statistics for evaluating overall adequacy of risk prediction procedures with censored survival data," *Statistics in Medicine*, vol. 30, no. 10, pp. 1105–1117, 2011. [Online]. Available: <https://onlinelibrary.wiley.com/doi/abs/10.1002/sim.4154>
- [31] L. Buitinck, G. Louppe, M. Blondel *et al.*, "API design for machine learning software: experiences from the scikit-learn project," in *ECML PKDD Workshop: Languages for Data Mining and Machine Learning*, 2013, pp. 108–122.
- [32] C. Davidson-Pilon, "lifelines: survival analysis in python," *Journal of Open Source Software*, vol. 4, no. 40, p. 1317, 2019. [Online]. Available: <https://doi.org/10.21105/joss.01317>
- [33] H. Wickham, *ggplot2: Elegant Graphics for Data Analysis*. Springer-Verlag New York, 2016. [Online]. Available: <https://ggplot2.tidyverse.org>
- [34] F. Nogueira, "Bayesian optimization: Open source constrained global optimization tool for python," 2014-. [Online]. Available: <https://github.com/fmfn/BayesianOptimization>
- [35] Microsoft, "Neural Network Intelligence," 1 2021. [Online]. Available: <https://github.com/microsoft/nni>
- [36] S. J. Pan and Q. Yang, "A survey on transfer learning," *IEEE Transactions on knowledge and data engineering*, vol. 22, no. 10, pp. 1345–1359, 2009.
- [37] S. Yousefi, F. Amrollahi, M. Amgad *et al.*, "Predicting clinical outcomes from large scale cancer genomic profiles with deep survival models," *Scientific Reports*, vol. 7, no. 1, pp. 1–11, 2017.
- [38] R. K. Sevakula, V. Singh, N. K. Verma *et al.*, "Transfer learning for molecular cancer classification using deep neural networks," *IEEE/ACM transactions on computational biology and bioinformatics*, vol. 16, no. 6, pp. 2089–2100, 2018.
- [39] Z. Xu, J. Zhang, Q. Zhang *et al.*, "Explainable learning for disease risk prediction based on comorbidity networks," in *2019 IEEE International Conference on Systems, Man and Cybernetics (SMC)*. IEEE, 2019, pp. 814–818.